Supplementary Information (SI) for Journal of Materials Chemistry B.

Supplementary Information for

Bismuth-Functionalized Probiotics for Enhanced Antitumor Radiotherapy and Immune Activation

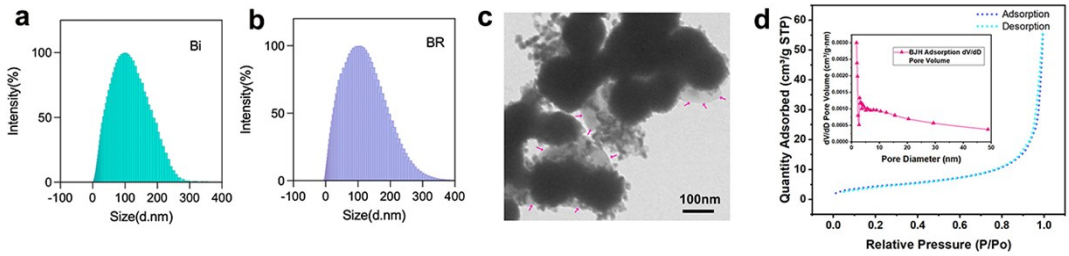

Figure S1. (a&b) Particle size distribution profiles of Bi and BR nanoparticles. (c) Polydopamine-coated bismuth nanoparticles. (d) BET adsorption-desorption curve and pore size distribution of bismuth-based nanoparticles.

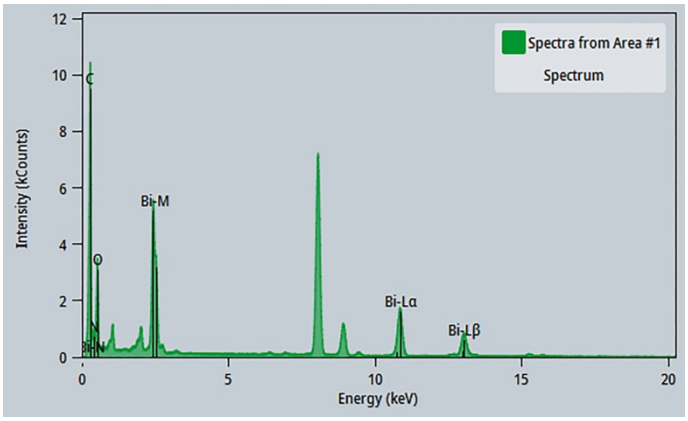

Figure S2. Bismuth element surface scan data of BPBR.

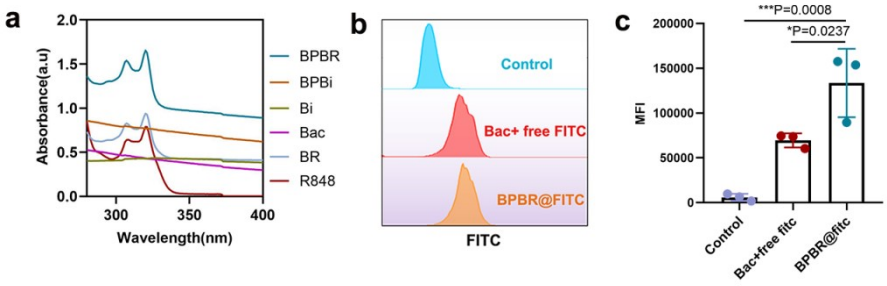

Figure S3. (a) UV-Vis spectrum. (b&c) Flow cytometry analysis of fluorescence intensity of BPBR@FITC and Bac+FITC (b) and corresponding fluorescence intensity quantification (c). Data are presented as mean values ± SD (n = 3). NS: no statistical significance, $^{*}P < 0.05$, $^{**}P < 0.01$, $^{***}P < 0.001$, $^{****}p < 0.0001$.

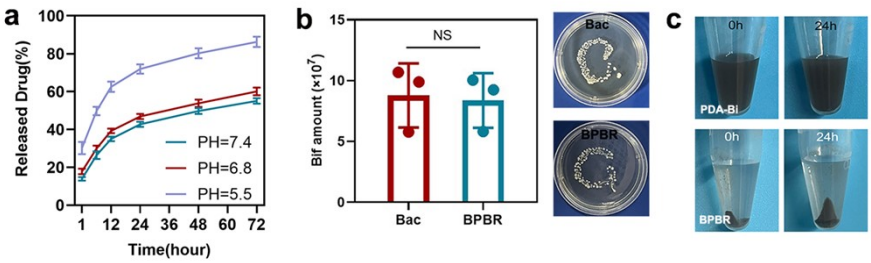

Figure S4. (a) In vitro release. (b) Bacterial growth after plating with BPBR and Bac. (c) Analysis images showing the stability of polydopamine-coated Bi NPs and BPBR. Data are presented as mean values ± SD (n = 3). NS: no statistical significance, $^{*}P < 0.05$, $^{**}P < 0.01$, $^{***}P < 0.001$, $^{****}p < 0.0001$. Significance between every two groups was calculated using the unpaired two-tailed Student's t test and one-way or two-way analysis of variance (ANOVA) was used for multiple comparisons.

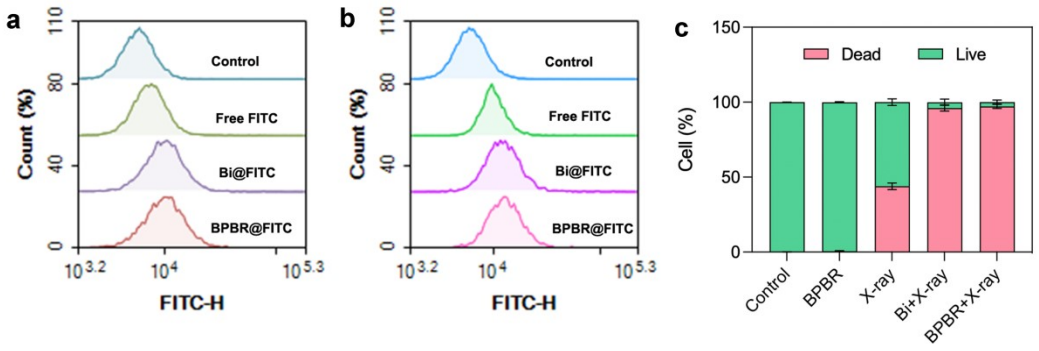

Figure S5. Flow cytometry analysis of fluorescence intensity of CT26 cells after 1 hour (a) and 4 hours (b) of uptake. (c) Quantitative analysis of live/dead staining.

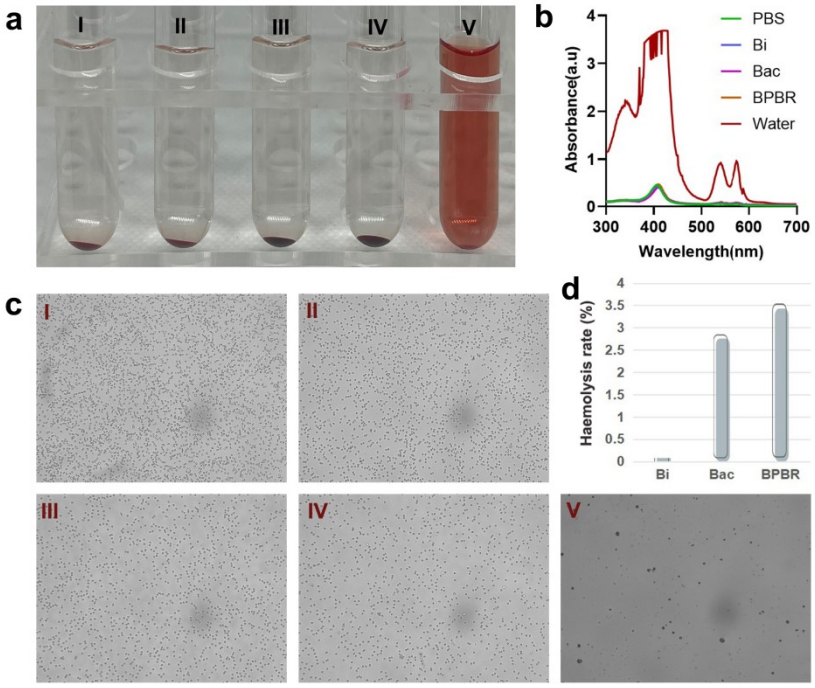

Figure S6. Hemolysis experiment. (a) Photographs of red blood cells after different treatments. (b) UV absorption spectra of red blood cells after different treatments. (c) Changes in red blood cells under a microscope after different treatments. (d) Hemolysis rate of each group. I: PBS; II: Bi; III: Bac; IV: BPBR; V: Water.

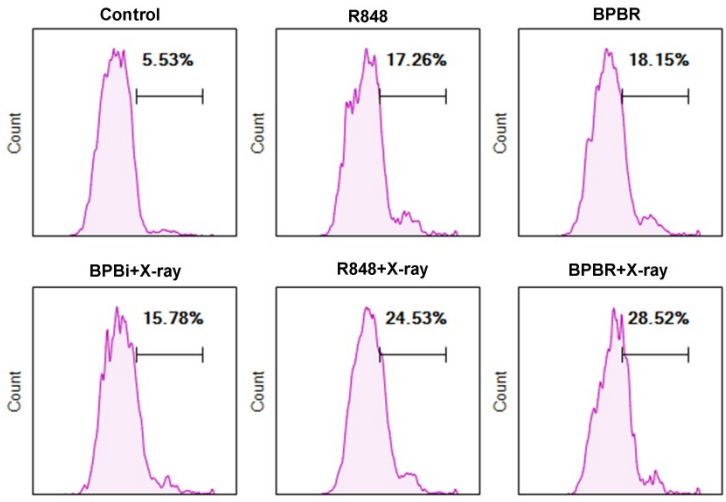

Figure S7. Phagocytosis rate of BMDC against CT26 cells.

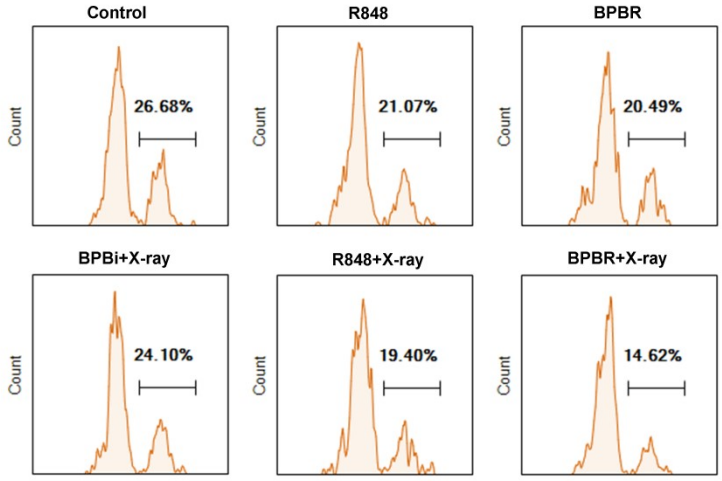

Figure S8. Proliferation rate of CT26 cells.

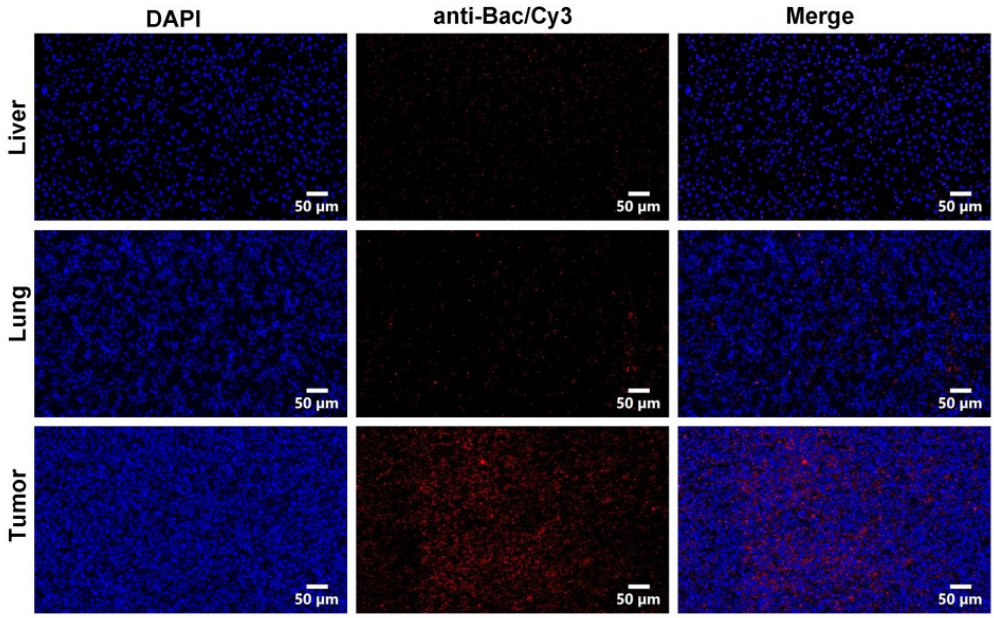

Figure S9. Localized sections of bacteria in the liver, kidney and tumor areas.

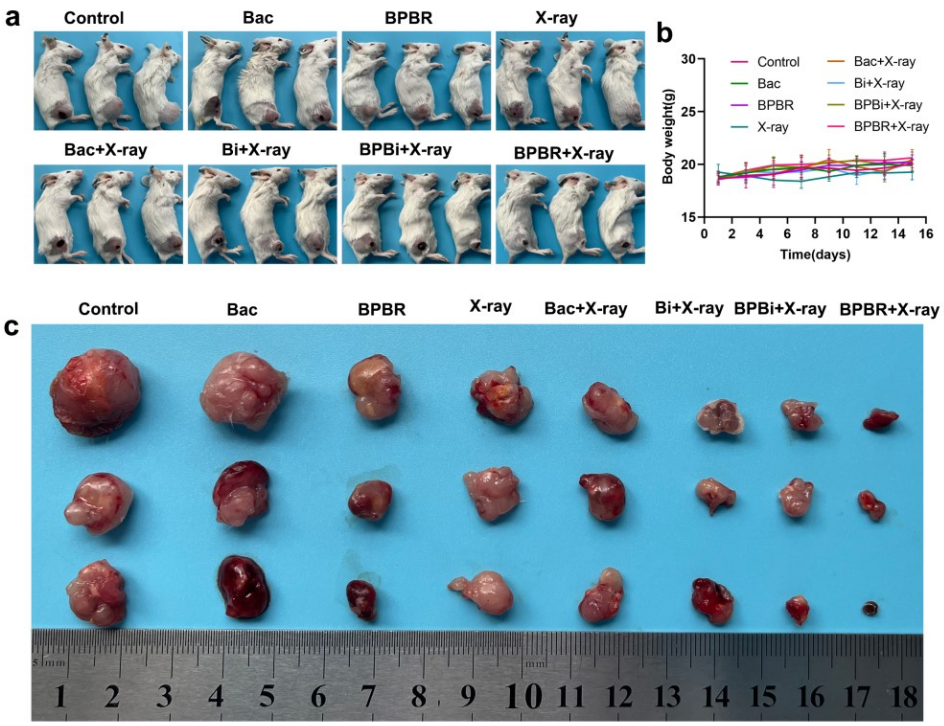

Figure S10. (a) Photos of 3 randomly selected mice from each group after treatment. (b) Body weight curves of mice in each group. (c) Dissection photos of tumors from 3 randomly selected mice from each group after treatment.

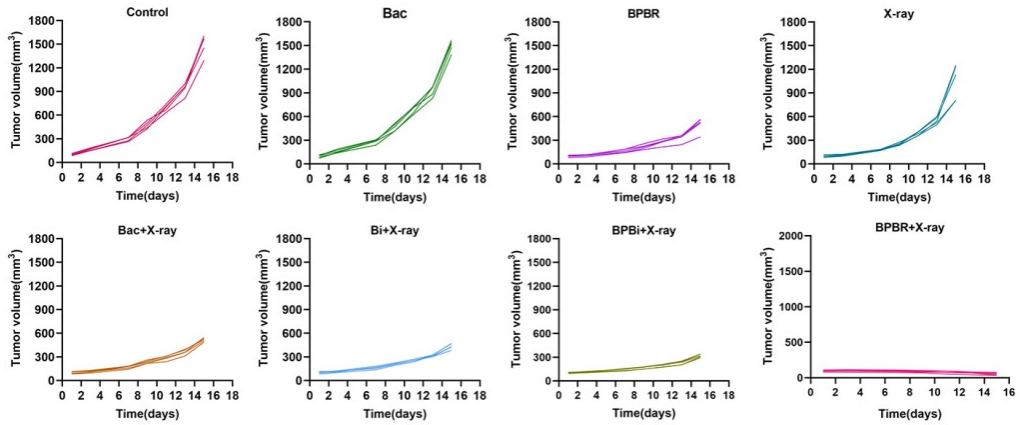

Figure S11. Tumor volume change curves of five mice in each group.

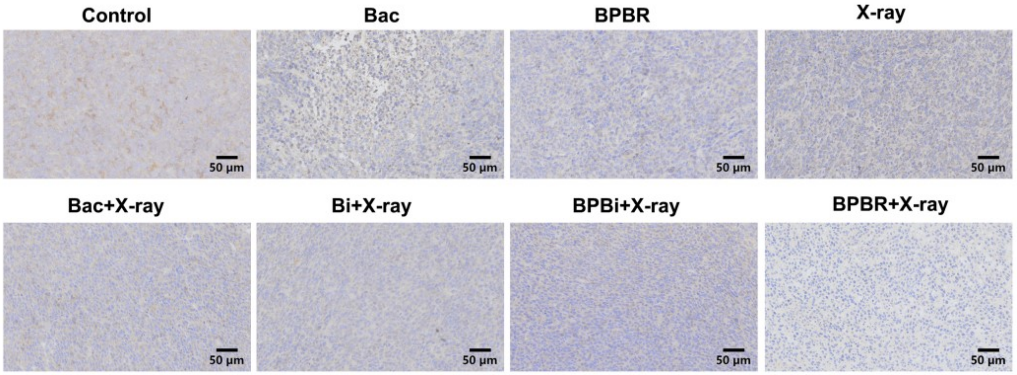

Figure S12. Expression of Hif-2α in tumors of each group.

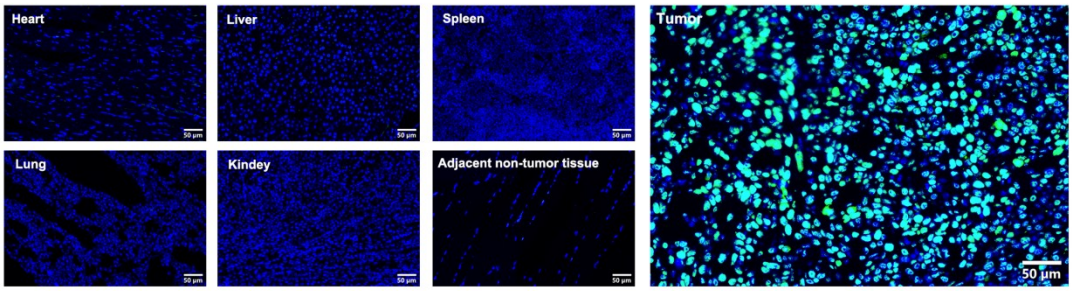

Figure S13. Immunofluorescence analysis of H_2AX expression in normal visceral organs (heart, liver, spleen, lung, kidney), peritumoral tissues, and tumor tissues.

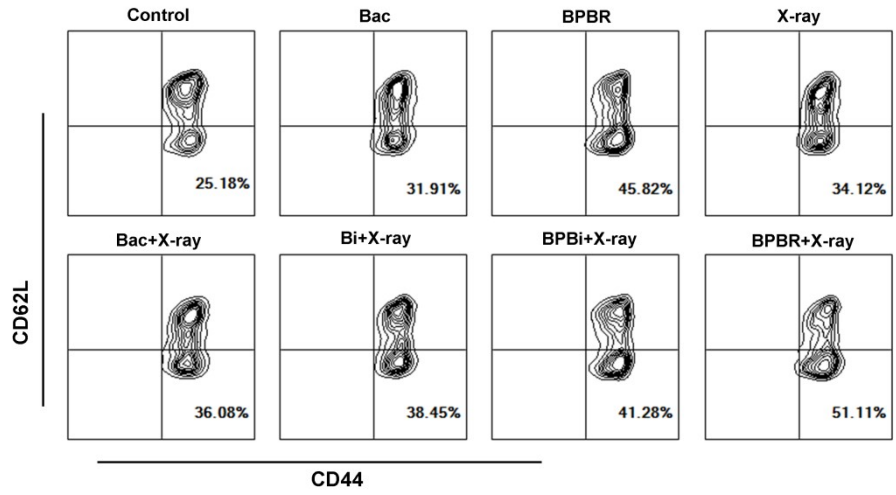

Figure S14. Flow cytometry analysis of the proportion of effector memory T cells (Tem, CD3+CD8+CD62L-CD44+) in the spleen of mice in each group.

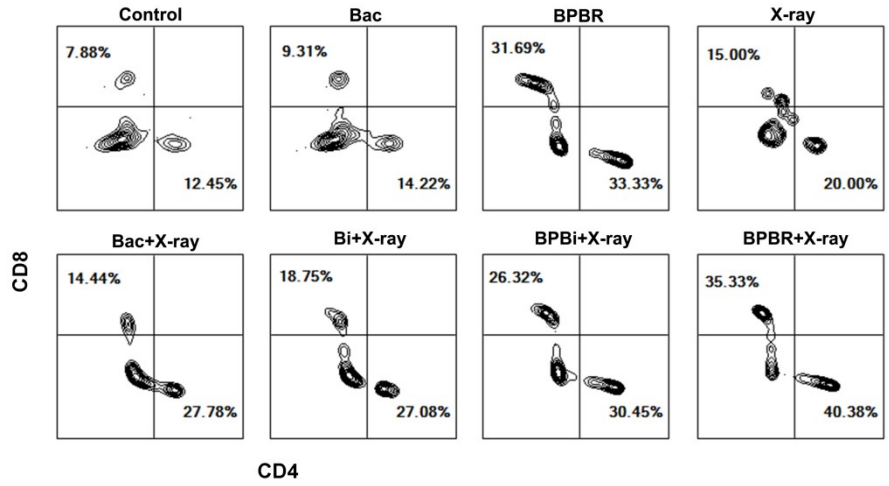

Figure S15. Flow cytometry analysis of the proportion of CD4+ T cells and CD8+ T cells in tumors of mice in each group.

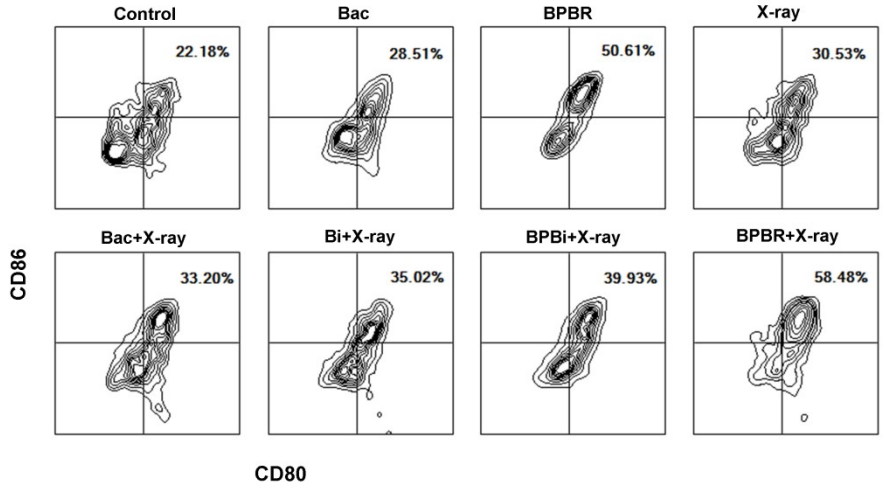

Figure S16. Flow cytometry analysis of the proportion of mature DC cells (CD11c+CD80+CD86+) in tumors of mice in each group.

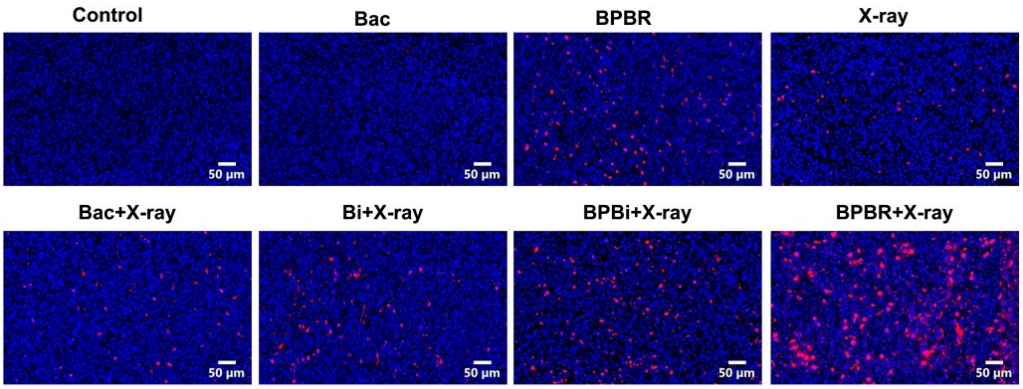

Figure S17. Immunofluorescence expression of CD8+ T cells in tumors of each group.

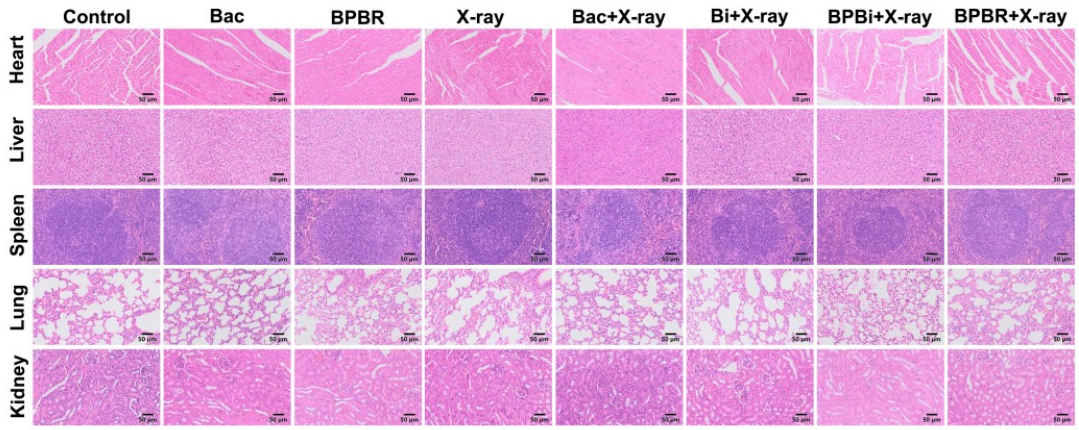

Figure S18. HE staining results of major organs (heart, liver, spleen, lung, and kidney) in each group.

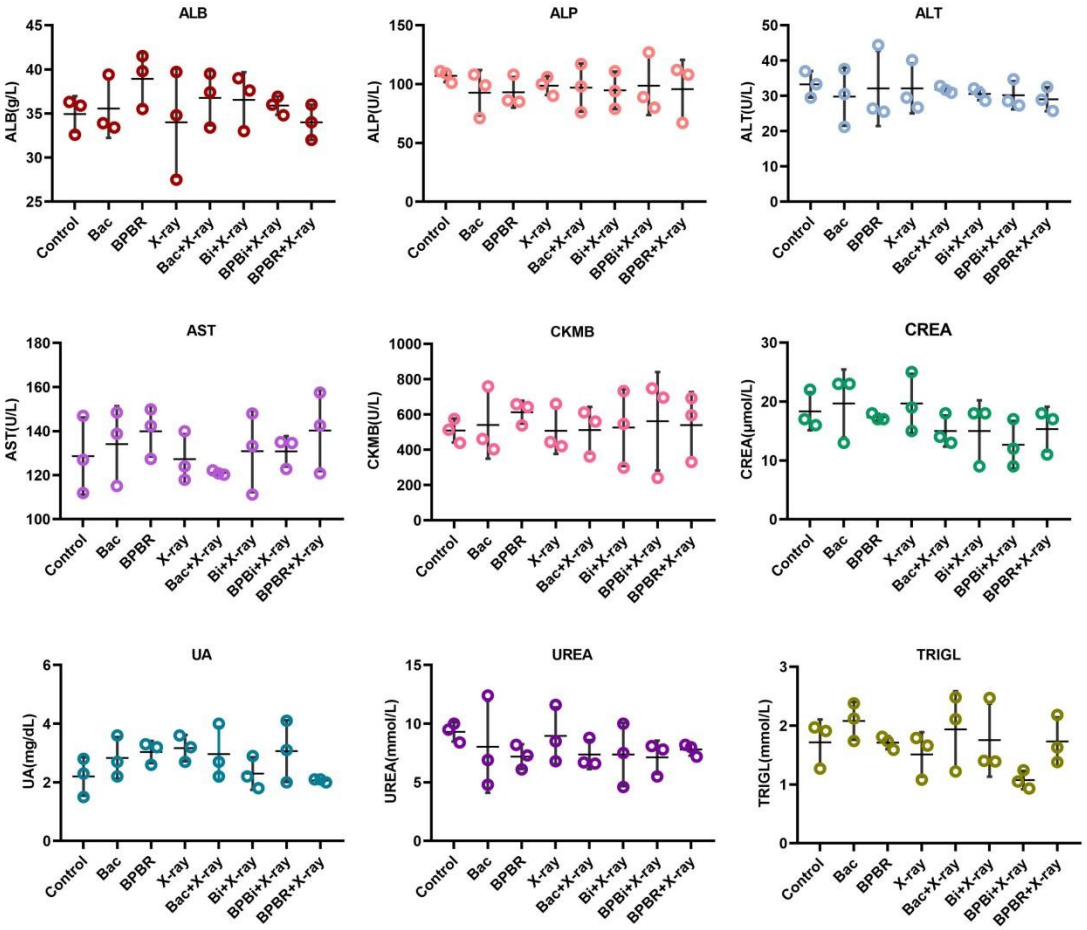

Figure S19. Blood biochemical analysis of mice in different treatment groups. ALB: albumin; ALP: alkaline phosphatase; ALT: alanine aminotransferase; AST: aspartate aminotransferase; CKMB: creatine kinase MB; CREA: creatinine; UA: uric acid; UREA: urea; TRIGL: triglycerides.